Biodistribution and Kinetics of Radiolabeled Proteins in Rats with Focal Infection

Wim J.G. Oyen, Roland A.M.J. Claessens, Jos W.M. van der Meer, and Frans H.M. Corstens

Departments of Nuclear Medicine and Internal Medicine, University Hospital Nijmegen, and Division of General Internal Medicine, Nijmegen, The Netherlands

The purpose of this study was to evaluate the role of both protein and radionuclide in the accumulation of ^{111}In-labeled human immunoglobulin G (IgG) in infectious foci. In rats with a calf muscle infection, biodistribution was determined 2, 6, 24, and 48 hr after injection of a radiopharmaceutical. For IgG, human serum albumin (HSA) and human immunoglobulin A (IgA), all labeled with ^{111}In, target-to-background (T/B) ratios were similar throughout the study. However, absolute abscess uptake of ^{111}In-IgA was significantly lower. For IgG labeled with ^{111}In, ^{123}I, or ^{99m}Tc, similar T/B ratios were found up to 24 hr. After 48 hr, the T/B ratio of ^{111}In-IgG was significantly higher than the T/B ratio of ^{123}I-IgG. The absolute abscess uptake of ^{111}In-IgG was higher than that of ^{99m}Tc-IgG at 24 hr and ^{123}I-IgG at 48 hr. In conclusion, the radionuclide appears to be of major importance in the accumulation of radiolabeled proteins in infectious foci. Protein mainly influences blood clearance and distribution in organs. The Fc-γ receptor is not crucial for accumulation in infectious foci.

J Nucl Med 1992; 33:388–394

Several reports suggest the utility of scintigraphy with ^{111}In-labeled nonspecific polyclonal human immunoglobulin G (^{111}In-IgG) for the detection of various types of focal infection in humans (*1–4*). However, the mechanism of ^{111}In-IgG accumulation in infectious and noninfectious inflammatory foci is not fully understood. Both specific receptor interaction and nonspecific macromolecular entrapment have been proposed (*5–8*). To evaluate the role of the type of protein in the mechanism of ^{111}In-IgG accumulation in infectious foci, ^{111}In-IgG was compared to ^{111}In-labeled human serum albumin (HSA), and ^{111}In-labeled human immunoglobulin A (IgA); also ^{123}I-IgG was compared to ^{131}I-HSA. To elucidate the role of the radionuclide and corresponding labeling method, IgG was labeled with ^{111}In, ^{123}I and ^{99m}Tc and HSA was radiolabeled with ^{111}In and ^{131}I.

Received Jun. 6, 1991; revision accepted Oct. 8, 1991.

For reprints contact: Wim J.G. Oyen, MD, Department of Nuclear Medicine, University Hospital Nijmegen, P.O. Box 9101, 6500 HB Nijmegen, The Netherlands.

MATERIALS AND METHODS

Radiopharmaceuticals

The biodistribution and kinetics of six radiolabeled proteins were studied.

Indium-111-IgG. (IgG: Sandoglobulin, Sandoz AG, Nuernberg, FRG). Diethylenetriaminepentaacetic bicyclic anhydride (bicyclic DTPA) was conjugated to the protein according to Hnatowich and colleagues (*9*). The number of DTPA ligands, conjugated to one protein molecule was determined by the method described by Hnatowich et al. (*9*). The purified DTPA-conjugated protein was diluted to 2 mg/ml with 0.15 *M* acetate (pH = 6.5) and sterilized by membrane filtration. Aliquots of 0.5 ml of the conjugate were radiolabeled with ^{111}In (Indium chloride, Amersham International Ltd., Buckinghamshire, UK) via citrate transchelation. The radiochemical purity of all radiopharmaceuticals was determined by instant thin-layer chromatography (ITLC) on Gelman ITLC-SG strips (Gelman Laboratories, Ann Arbor, MI) with 0.1 *M* citrate (pH = 5) as solvent. Labeling efficiency was checked batchwise by HPLC on an ^{125}I size exclusion column (Waters-Millipore) with a 0.1 *M* acetate buffer (pH = 6) as solvent. A dose of 10 μg, labeled with 2 MBq ^{111}In, was injected intravenously.

Iodine-123-IgG. (IgG: Sandoglobulin, Sandoz AG, Nuernberg, FRG). IgG was labeled with ^{123}I by means of the Iodo-gen method (Iodo-gen, 28600, Pierce, Rockford, IL) (*10*). Unbound iodine was removed with Sephadex 25. A dose of 10 μg IgG labeled with 3 MBq ^{123}I was injected intravenously.

Technetium-99m-IgG. Kits for labeling IgG with ^{99m}Tc (Technescan-HIG) were kindly provided by Mallinkcrodt Diagnostica Holland, Petten, The Netherlands. A kit, containing 1 mg of 2-iminothiolane-derivatized IgG (obtained from the Central Laboratory of the Bloodtransfusion Service of The Netherlands Red Cross, Amsterdam, The Netherlands) and stannous chloride, was radiolabeled with 500 MBq ^{99m}Tc eluate. In vitro stability was tested by HPLC analysis after in-vitro storage of ^{99m}Tc-IgG at 37°C for 24 hr. A dose of 10 μg, labeled with 4 MBq ^{99m}Tc, was injected intravenously.

Indium-111-HSA. (Human Albumin 20%, Central Laboratory of the Bloodtransfusion Service of The Netherlands Red Cross, Amsterdam, The Netherlands). DTPA-conjugation and ^{111}In labeling were accomplished as described above. A dose of 10 μg, labeled with 2 MBq ^{111}In, was injected intravenously.

Iodine-131-HSA. (Medgenix Diagnostics, Fleurus, Belgium). The radiopharmaceutical was obtained commercially. The protein bound ^{131}I activity was 96%. A dose of 40 μg labeled with 0.5 MBq ^{131}I was administered intravenously.

Indium-111-IgA. (Human IgA, I1010, Sigma Chemical Company, St. Louis, MO). DTPA-conjugation and ^{111}In labeling were

accomplished as described above. IgA activity was determined before and after conjugation with DTPA by immunoelectrophoresis. Non-IgA bound ^{111}In was removed with Sephadex PD 10. A dose of 10 μg, labeled with 2 MBq ^{111}In, was injected intravenously.

Animals and Study Design

A calf muscle abscess was induced in young, male, randomly bred Wistar rats (weight 200-220 g) after ether anesthesia with approximately 2×10^8 colony-forming units of *Staphylococcus aureus* in 0.1 ml 50:50% suspension of autologous blood and normal saline. The animals were randomly divided in groups.

Twenty-four hours after the inoculation of *Staphylococcus aureus* in the muscle, when swelling of the muscle was apparent, the respective radiopharmaceuticals were injected in the tail vein.

To collect tissues, rats were killed with 30 mg intraperitoneally injected phenobarbital, followed by cervical dislocation at 2, 6, 24, and 48 hr after injection. For ^{99m}Tc-IgG, tissues were obtained up to 24 hr p.i. Each peptide was evaluated in six animals at each time point. Samples of bone marrow (taken from the right femur), blood, and urine were collected. The infected left calf muscle, the right calf muscle, the liver, the spleen, the kidneys, and the right femur were collected and blotted dry. The activity in the tissues and samples was measured in a shielded well-type gamma counter. The excreted activity in feces and urine of each peptide at each time point between injection of the radiopharmaceutical and killing of the animals was also measured in the well counter. To correct for radioactive decay and permit calculation of the uptake of the radiopharmaceuticals in each organ as a fraction of the injected dose, aliquots of the respective doses were counted simultaneously. The measured activity in tissues and samples was expressed as percentage of injected dose per gram (%ID/g) and the excreted activity per animal as percentage of total dose administered.

For calculation of background activity, we used a combination of normal muscle activity and blood activity. Since the blood volume of rats approximates 60 ml per kg bodyweight (6%), 94% × the activity per gram in muscle plus 6% × the activity per gram in blood was adopted as the value for background activity (*11*). Abscess-to-background ratios were calculated.

Statistical Analysis.

All mean values are given ± s.e.m. Statistical analysis was performed using Tukey's analysis of variance. The level of significance was set at 0.05.

RESULTS

Labeling Effiency and Characterization of Proteins

Conjugation of DTPA to proteins resulted in two to three DTPA ligands per protein molecule. For ^{111}In-IgG, labeling efficiency was 95%. ITLC and HPLC analysis results were similar. In patients, all ^{111}In activity in blood samples was still protein-bound at 48 hr p.i. No cell binding of ^{111}In could be detected.

For ^{123}I-IgG, radiochemical purity was 98% after removing unbound iodine. For ^{99m}Tc-IgG, labeling efficiency was 99%. HPLC analysis showed that approximately 75% of the original ^{99m}Tc activity was still protein-bound after 24 hr in vitro.

For ^{111}In-HSA and ^{131}I-HSA, the protein bound activity was 99% and 96%, respectively.

IgA activity after conjugation with DTPA was 89% of the original activity. Indium-111-IgA labeling efficiency was 96% after purification.

Role of Protein

Comparison of In-111-IgG, In-111-HSA and In-111-IgA. Figure 1 shows that all radiopharmaceuticals had a higher accumulation in the infectious focus than in the contralateral normal muscle at all sampling times. Indium-111-IgG uptake in the abscesses remained at a constant, high level. Although not significant, both ^{111}In-HSA and ^{111}In-IgA showed a tendency to decrease over time. The uptake of ^{111}In-IgG and ^{111}In-HSA in the abscess revealed no significant differences. Indium-111-IgA uptake was significantly lower at all points in time ($p < 0.05$). However, abscess-to-background ratios of all ^{111}In-labeled proteins (Fig. 2) did not differ significantly.

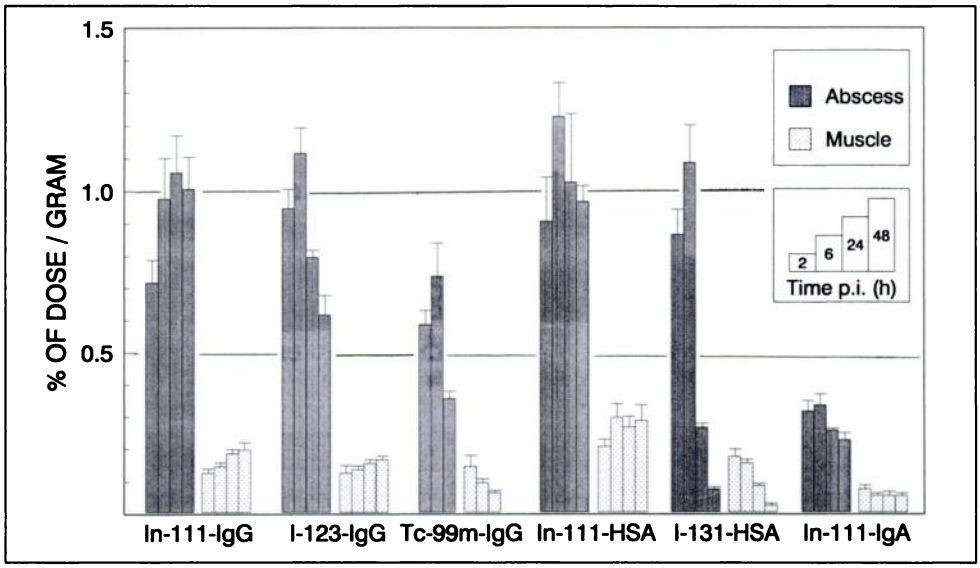

FIGURE 1. Activity uptake in abscess and muscle, expressed as %dose/g (error bars indicate s.e.m.).

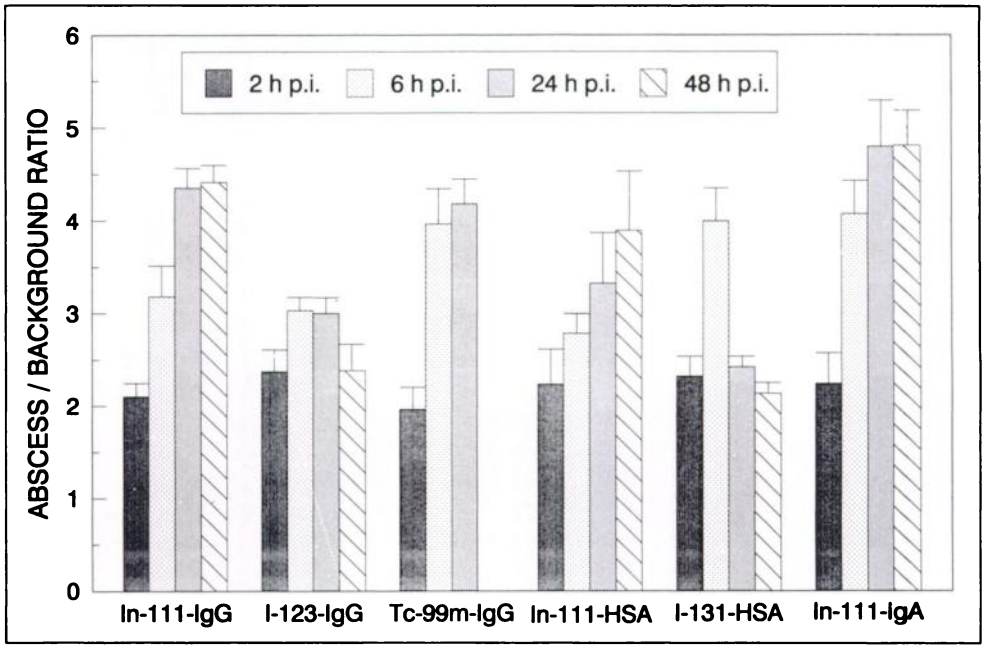

FIGURE 2. Abscess to background ratios (error bars indicate s.e.m.).

After 6 hr, ^{111}In-IgG cleared significantly slower from the blood than ^{111}In-HSA, $p < 0.05$ (Fig. 3). The blood concentration of ^{111}In-IgA was significantly lower than that of ^{111}In-IgG and ^{111}In-HSA at each time point ($p < 0.05$).

Table 1 and Figure 4 show the distribution in various organs. Indium-111-IgA showed marked accumulation in the kidneys, liver and spleen. Indium-111-IgG and ^{111}In-HSA uptake in the liver and the spleen did not differ significantly. However, renal uptake of ^{111}In-IgG was significantly higher compared to ^{111}In-HSA ($p < 0.05$).

Excretion of ^{111}In-IgG and ^{111}In-HSA were also similar (Fig. 5). Indium-111-IgA excretion was slightly higher.

Comparison of ^{123}I-IgG and ^{131}I-HSA. At 24 and 48 hr, both ^{123}I-IgG and ^{131}I-HSA revealed significant washout from the abscess, $p < 0.05$ (Fig. 1). The absolute abscess uptake of ^{123}I-IgG was significantly higher than the corresponding uptake of ^{131}I-HSA at 24 and 48 hr, since the washout of ^{123}I-IgG was slower than that of ^{131}I-HSA ($p < 0.05$). This also applied for the absolute muscle uptake. For this reason, abscess-to-background ratios of the two iodinated proteins did not differ (Fig. 2).

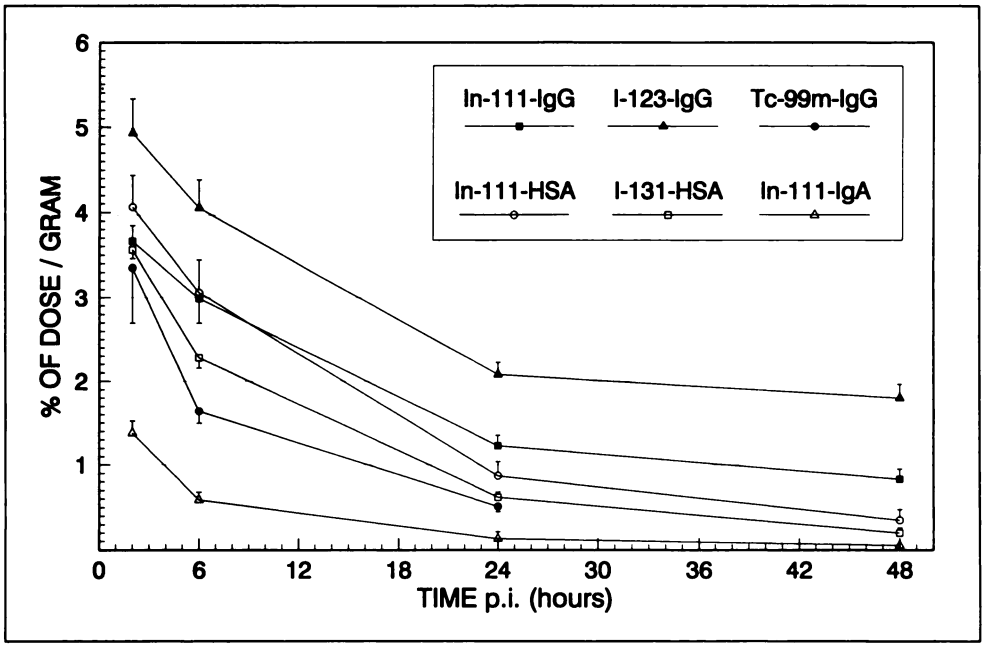

FIGURE 3. Blood activity, expressed as %dose/g (error bars indicate s.e.m.).

TABLE 1
Biodistribution, Expressed as Percentage of Administered Dose per Gram (Mean Values ± s.e.m.)

Organ	Time	^{111}In-IgG	^{123}I-IgG	^{99m}Tc-IgG	^{111}In-HSA	^{131}I-HSA	^{111}In-IgA
Liver	2	1.14 ± 0.03	0.92 ± 0.11	0.88 ± 0.03	1.07 ± 0.16	0.54 ± 0.04	6.25 ± 0.12
	6	1.32 ± 0.07	0.66 ± 0.10	0.77 ± 0.07	1.39 ± 0.19	0.42 ± 0.02	6.94 ± 0.34
	24	1.37 ± 0.09	0.26 ± 0.02	0.38 ± 0.08	1.29 ± 0.19	0.12 ± 0.00	5.94 ± 0.19
	48	1.49 ± 0.04	0.29 ± 0.03	—	1.47 ± 0.21	0.05 ± 0.01	4.85 ± 0.33
Spleen	2	1.09 ± 0.04	0.90 ± 0.10	0.88 ± 0.08	1.12 ± 0.13	0.58 ± 0.05	4.77 ± 0.59
	6	1.43 ± 0.10	0.72 ± 0.08	0.77 ± 0.08	1.68 ± 0.15	0.44 ± 0.03	3.70 ± 0.36
	24	1.61 ± 0.09	0.36 ± 0.02	0.40 ± 0.02	1.90 ± 0.31	0.12 ± 0.01	4.41 ± 0.60
	48	1.81 ± 0.11	0.28 ± 0.02	—	2.14 ± 0.19	0.05 ± 0.00	3.15 ± 0.48
Kidneys	2	4.18 ± 0.22	1.47 ± 0.14	9.41 ± 0.84	1.57 ± 0.17	0.93 ± 0.09	7.64 ± 0.20
	6	5.45 ± 0.49	1.15 ± 0.08	11.10 ± 0.96	1.62 ± 0.15	0.70 ± 0.03	7.88 ± 0.13
	24	5.38 ± 0.46	0.56 ± 0.03	10.15 ± 0.81	1.74 ± 0.18	0.21 ± 0.01	8.27 ± 0.14
	48	5.36 ± 0.61	0.45 ± 0.03	—	2.50 ± 0.31	0.09 ± 0.01	7.81 ± 0.25
Bone marrow	2	1.01 ± 0.10	1.30 ± 0.10	1.27 ± 0.28	1.19 ± 0.07	0.90 ± 0.17	1.14 ± 0.08
	6	1.45 ± 0.08	0.99 ± 0.11	0.78 ± 0.09	1.13 ± 0.18	0.68 ± 0.05	0.99 ± 0.06
	24	1.40 ± 0.08	0.40 ± 0.03	0.27 ± 0.01	1.24 ± 0.02	0.20 ± 0.05	0.89 ± 0.07
	48	1.40 ± 0.08	0.39 ± 0.02	—	1.07 ± 0.10	0.06 ± 0.01	0.79 ± 0.09
Bone	2	0.25 ± 0.02	0.27 ± 0.02	0.22 ± 0.03	0.28 ± 0.04	0.24 ± 0.02	0.18 ± 0.02
	6	0.23 ± 0.02	0.23 ± 0.02	0.16 ± 0.01	0.37 ± 0.04	0.18 ± 0.03	0.14 ± 0.01
	24	0.28 ± 0.02	0.11 ± 0.01	0.08 ± 0.00	0.39 ± 0.05	0.10 ± 0.01	0.16 ± 0.02
	48	0.34 ± 0.05	0.10 ± 0.01	—	0.47 ± 0.09	0.08 ± 0.00	0.11 ± 0.01

The blood clearance and excretion rate of ^{123}I-IgG were significantly slower than the clearance and excretion rate of ^{131}I-HSA $p < 0.05$ (Fig. 3 and 5). The accumulation in organs was significantly lower for ^{131}I-HSA than for ^{123}I-IgG, $p < 0.05$ (Table 1 and Fig. 4).

Role of Radionuclide

Comparison of ^{111}In-IgG, ^{123}I-IgG, and ^{99m}Tc-IgG. As shown in Figure 1, absolute abscess uptake over time showed different patterns for these labels: ^{111}In-IgG was relatively high and constant from 6 hr p.i. onwards; ^{123}I-IgG was also high at 6 hr p.i., but decreased afterwards; ^{99m}Tc-IgG was relatively low and decreased between 6 and 24 hr p.i. The uptake of ^{111}In-IgG in the abscess was significantly higher than that of ^{99m}Tc-IgG at 24 hr ($p < 0.05$). Also, at 48 hr there was more ^{111}In-IgG than ^{123}I-IgG activity in the abscess ($p < 0.05$). Abscess uptake of ^{123}I-IgG was initially significantly higher than that of ^{99m}Tc-IgG ($p < 0.05$), but did not differ significantly at 24 hr p.i. With regard to the abscess-to-background ratios (Fig. 2), only the higher ratio at 48 hr p.i. of ^{111}In-IgG compared to the ratio of ^{123}I-IgG reached a level of significance ($p < 0.05$).

As shown in Figure 3, significant differences could be noted in blood clearance: ^{99m}Tc-IgG showed the fastest clearance ($p < 0.05$) and ^{123}I-IgG the slowest ($p < 0.05$).

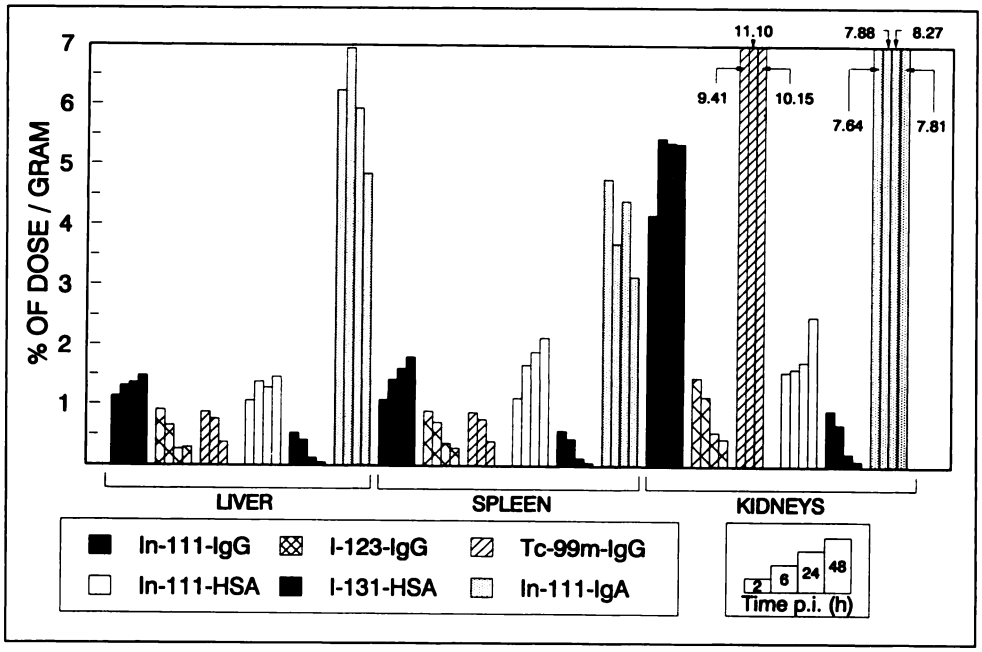

FIGURE 4. Biodistribution in liver, kidney, and spleen.

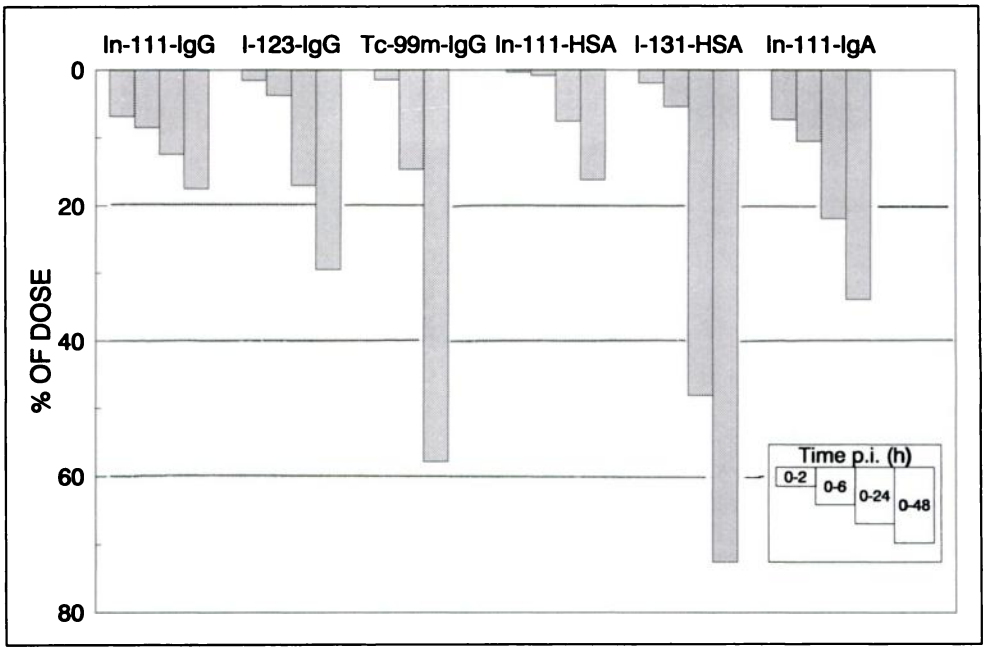

FIGURE 5. Cumulative excretion of activity, expressed as %dose.

The accumulation of the three IgG preparations in the kidneys varied significantly: ^{123}I-IgG had the lowest ($p < 0.05$) and ^{99m}Tc-IgG had the highest uptake ($p < 0.05$) (Table 1 and Figure 4). In liver, spleen, bone and bone marrow, ^{111}In-IgG uptake significantly exceeded ^{123}I-IgG and ^{99m}Tc-IgG uptake ($p < 0.05$). Indium-111-IgG showed stable or increasing activity over time in liver, spleen, kidneys, bone marrow and bone. Iodine-123-IgG activity decreased in these organs, while ^{99m}Tc-IgG activity also decreased in these organs with the exception of the kidneys, whose activity remained relatively stable. Typically, the bone marrow uptake exceeded the bone uptake by a factor four to five for all preparations.

As shown in Figure 5, approximately 20% of the administered ^{111}In-IgG was excreted in faeces and urine within 48 hr, excretion of ^{123}I-IgG was higher (approximately 30%). After administration of ^{99m}Tc-IgG approximately 60% of the radiopharmaceutical was excreted within 24 hr.

Comparison of ^{111}In-HSA and ^{131}I-HSA. Similar differences as noted between ^{111}In-IgG and ^{123}I-IgG were found between ^{111}In-HSA and ^{131}I-HSA: retention in the abscess, constant abscess to background ratios over time, significant accumulation in organs, and low excretion rate of ^{111}In-HSA versus washout from the abscess, over time decreasing abscess-to-background ratios, low organ uptake, and high excretion rate of ^{131}I-HSA.

DISCUSSION

The similar abscess uptake and abscess to background ratios of ^{111}In-IgG and ^{111}In-HSA at various time points indicate that specific receptor binding of labeled IgG in an infectious focus, if at all present, is not the major factor in accumulation of labeled IgG in such a focus, since HSA lacks this receptor affinity. These findings are in concert with the autoradiographic studies by Morrel et al. and our own experience in neutropenic patients (7,8).

IgA is an immunoglobulin without Fc-γ receptor affinity. On inflammatory cells few Fc-α receptors are present (*12*). However, target-to-background ratios of ^{111}In-IgA in infections in extremities do not differ from those after ^{111}In-IgG injection, thus confirming that Fc-γ receptor interaction is not a major factor in the accumulation of ^{111}In-IgG in infectious foci. The different uptake in liver, spleen and kidney of ^{111}In-IgG and ^{111}In-IgA revealed that protein is also a major factor in biodistribution. Since hepatocytes of rats are equipped with IgA receptors, the high liver uptake of ^{111}In-IgA in our experiment is not surprising (*13*). The initially high and persistent organ uptake of ^{111}In-IgA is in accordance with fast clearance from the blood to the organs. Hepatic, renal and splenic uptake of ^{111}In-IgA are so high, that, at least in rats, this agent is not suited for imaging infectious foci in these areas. The differences observed between ^{111}In-IgG and ^{111}In-IgA confirm the results of Fischman et al., who noted that physical chemical differences between ^{111}In-labeled Fab and Fc fragments of IgG might account for differences in abscess localization and biodistribution (*14*).

More striking differences were observed with regard to the biological behavior of IgG when it was labeled to either ^{111}In, ^{123}I or ^{99m}Tc. Indium-111-IgG was retained in the abscess, while ^{123}I-IgG and ^{99m}Tc-IgG showed washout. The physiological uptake in organs of ^{111}In-IgG, the radiopharmaceutical thus far most frequently used in patient studies, is relatively high for most organs, compared to ^{123}I-IgG and, except for kidney uptake, ^{99m}Tc-IgG.

The relatively slow blood clearance of ^{123}I-IgG might appear disadvantageous in detection of infectious foci, because of persistingly high background activity. The most probable explanation for this persisting blood activity is

dehalogenation of the protein in organs and subsequent washin of iodine and iodinated fragments into the circulation. A labeling procedure with more stable halogenation could overcome both this problem as well as washout of iodinated IgG from the infectious focus over time. The low physiological uptake in organs of ^{123}I-IgG could be useful for the evaluation of infectious foci in parenchymatous organs. Clinical studies with ^{111}In-IgG showed disappointing results for the detection of infectious foci in these organs (*4,8*). Additional advantages of ^{123}I are its physical properties: a half-life of 13 hr which permits imaging up to 48 hr after administration, a relatively low radiation burden per unit activity compared to ^{111}In, thus allowing a higher dose to administer leading to high quality imaging with reasonable imaging times. A somatic dose equivalent of 15 mSv after injection of 75 MBq ^{111}In-IgG necessitates reluctancy in the use of this radiopharmaceutical in pediatric patients (*15*). The more favorable distribution of ^{123}I-IgG in this animal study compared to ^{111}In-IgG might bring IgG scintigraphy in scope for imaging of infection in children. Major drawbacks for widespread use of ^{123}I-IgG are of course its limited availability and high cost.

Technetium-99m-IgG performs well up to 6 hr p.i. Although the abscess-to-background ratio remained at the same high level after 24 hr p.i., a rapid decrease of abscess activity was apparent. This decrease in combination with a physical half-life of 6 hr is a major impediment to obtaining good quality images after 24 hr. One might wonder whether or not this decrease makes ^{99m}Tc-IgG scintigraphy less suited for the detection of subacute and low-grade infections in humans, in whom 48-hr images are often necessary to achieve good sensitivity (*3*). The high renal uptake and excretion of ^{99m}Tc-IgG, which was also observed by Rubin et al. for ^{99m}Tc-HSA, may interfere with abdominal imaging (*16*). Nevertheless, first results in humans with ^{99m}Tc-IgG, using the type of kit as in the present study, were encouraging (*17*). However, the design of the study by Buscombe was not ideal because of coinjection of ^{99m}Tc-IgG and ^{111}In leukocytes, leading possible interference of ^{111}In photons in the late ^{99m}Tc images. Moreover, ^{111}In-leukocyte scintigraphy was used as the golden standard. In a recent comparative study between ^{111}In-IgG and ^{111}In-labeled leukocyte scintigraphy, we found that in certain types of infection ^{111}In-labeled leukocyte scintigraphy was not suited as the golden standard (*4*). Recently, Abrams et al. reported a new ^{99m}Tc labeling method of proteins, using nicotinyl hydrazine derivative IgG (*18*). These investigators observed equivalent biodistribution of the ^{99m}Tc-labeled IgG preparation and ^{111}In-IgG. The fact that ^{99m}Tc-labeled nicotinyl hydrazine derivative IgG showed no washout from the abscess is of major importance for adequate imaging of acute infection with ^{99m}Tc-IgG. Further studies are needed to establish whether or not imaging up to 24 hr is sufficient to adequately reveal subacute and low-grade infection in humans.

Both the present study and data in the literature stress the relevance of the radiolabel on the dynamic distribution of the protein. In the present study, great similarity was observed between ^{111}In-IgG and ^{111}In-HSA. Although washout of ^{123}I-IgG from the abscess was slower than that of ^{131}I-HSA, both iodinated proteins showed similar trends with regard to uptake and retention in the abscess and the organs and the abscess-to-background ratios and distribution. In contrast, Calame et al. observed lower abscess-to-background ratios for ^{99m}Tc-HSA than for HSA-IgG (*19*). However, their experimental model differed from ours with regard to the animal, the strain of bacteria and amount of bacteria injected.

In conclusion, both the radionuclide and the protein are important in the biodistribution and kinetics of radiolabeled proteins used for detection of infectious foci. For accumulation in infectious foci, the radionuclide appears to be the major determinant. Specific Fc-γ receptor binding is probably of minor, if any, importance in the uptake of radiolabeled proteins in infectious foci. Most probably accumulation in these areas is caused by increased vascular permeability initially and retention with time by macromolecular entrapment. The protein defines the blood clearance and the distribution in organs of radiolabeled proteins, thus determining the amount of labeled protein that is available for delivery to an infectious focus.

Given the similarity of ^{111}In-IgG and ^{111}In-HSA in this animal model, further studies in humans with ^{111}In-HSA would be useful. Despite economic and logistic disadvantages, ^{123}I-IgG also merits further investigation. The present study warrants further studies to develop a radiolabeled protein with persistingly high abscess uptake, low background activity, fast blood clearance and low physiological organ uptake (*20*).

ACKNOWLEDGMENTS

The authors express their gratitude to: Mr. W. Tax, PhD (University Hospital Nijmegen, Department of Internal Medicine, Division of Nephrology) for his advice; Mr. G. Borm, PhD (University of Nijmegen, Department of Medical Statistics) for performing the statistical analysis; Mr. Gerrie Grutters and Mr. Hennie Eijkholt (University of Nijmegen, Central Animal Laboratory) and Mr. Emile Koenders and Mrs. Marjo van de Ven (University Hospital Nijmegen, Department of Nuclear Medicine) for technical assistance.

REFERENCES

1. Rubin RH, Fischman AJ, Callahan RJ et al. In-111-labeled nonspecific immunoglobulin scanning in the detection of focal infection. *N Engl J Med* 1989;321:935–940.
2. LaMuraglia GM, Fischman AJ, Strauss HW, et al. Utility of indium-111-labeled human immunoglobulin G scan for the detection of focal vascular graft infection. *J Vasc Surg* 1989;10:20–28.
3. Oyen WJG, Claessens RAMJ, van Horn JR, van der Meer JWM, Corstens FHM. Scintigraphic detection of bone and joint infections with indium-111-labeled nonspecific polyclonal human immunoglobulin G. *J Nucl Med* 1990;31:403–412.
4. Oyen WJG, Claessens RAMJ, van der Meer JWM, Corstens FHM. Detection of subacute infectious foci with indium-111-labeled autologous leu-

kocytes and indium-111-labeled human nonspecific immunoglobulin G: a prospective comparative study. *J Nucl Med* 1991;32:1854–1860.
5. Fischman AJ, Rubin RH, Khaw BA, et al. Detection of acute inflammation with ^{111}In-labeled nonspecific polyclonal IgG. *Semin Nucl Med* 1988; 18:335–344.
6. Rubin RH, Young LS, Hansen P, et al. Specific and nonspecific imaging of localized Fisher immunotype 1 pseudomonas aeruginosa infection with radiolabeled monoclonal antibody. *J Nucl Med* 1988;29:651–656.
7. Morrel EM, Tompkins RG, Fischman AJ, et al. Autoradiographic method for quantitation of radiolabeled proteins in tissues using indium-111. *J Nucl Med* 1989;30:1538–1545.
8. Oyen WJG, Claessens RAMJ, Raemaekers JMM, de Pauw BE, van der Meer JWM, Corstens FHM. Diagnosing infection in febrile granulocytopenic patients with indium-111 labeled human IgG. *J Clin Oncol* 1992:in press.
9. Hnatowich DJ, Childs RL, Lanteigne D, Najafi A. The preparation of DTPA-coupled antibodies radiolabeled with metallic radionuclides: an improved method. *J Immunol Meth* 1983;65:147–157.
10. Fraker PJ, Speck JC. Protein and cell membrane iodinations with a sparingly soluble chloramide, 1,3,4,6-tetrachloro-3α, 6-dephenylglycoluril. *Biochem Biophys Res Comm* 1978;80:849–857.
11. Jain NC. Blood volume and water balance. In: Jain NC, ed. *Schalm's veterinary hematology*, fourth edition. Philadelphia: Lea & Febiger; 1986:91.
12. Gorter A, Hiemstra PS, van der Voort EAM, van Es LA, Daha HR. Binding of human IgA1 to rat peritoneal macrophages. *Immunology* 1988; 69:207–212.
13. Underdown B, Schiff JM. Immunoglobulin A: strategic defense initiative at the mucosal surface. *Ann Rev Immunol* 1986;4:389–417.
14. Fischman AJ, Rubin RH, White JA et al. Localization of Fc and Fab fragments of nonspecific polyclonal IgG at focal sites of inflammation. *J Nucl Med* 1990;31:1199–1205.
15. Buijs WCAM, Oyen WJG, Claessens RAMJ, Koenders EB, Meeuwis APW, Corstens FHM. Biodistribution and radiation dosimetry of indium-111 labeled immunoglobulin G. [Abstract] *Eur J Nucl Med* 1990;16:433.
16. Rubin RH, Fischman AJ, Needleman M, et al. Radiolabeled, nonspecific, polyclonal human immunoglobulin in the detection of focal inflammation by scintigraphy: comparison with gallium-67-citrate and technetium-99m-labeled albumin. *J Nucl Med* 1989;30:385–389.
17. Buscombe JR, Lui D, Ensing G, de Jong R, Ell PJ. Tc-99m-human immunoglobulin (HIG)—first results of a new agent for the localization of infection and inflammation. *Eur J Nucl Med* 1990;16:649–655.
18. Abrams MJ, Juweid M, ten Kate CI et al. Technetium-99m-human polyclonal IgG radiolabeled via the hydrazino nicotinamide derivative for imaging focal sites of infection. *J Nucl Med* 1990;31:2022–2028.
19. Calame W, Feitsma HIJ, Ensing GJ et al. Detection of a local Staphylococcal infection in mice with technetium-99m-labeled polyclonal human immunoglobulin. *J Nucl Med* 1991;32:468–474.
20. Corstens FHM, van der Meer JWM. Chemotactic peptides: new locomotion for imaging of infection? *J Nucl Med* 1991;32:491–494.

EDITORIAL

Targeted Proteins for Diagnostic Imaging: Does Chemistry Make a Difference?

The imaging of occult infection is an important area of nuclear medicine. Vehicles for abscess localization have ranged from ^{67}Ga-citrate to radiolabeled leukocytes to radiolabeled immunoglobulin G (IgG) of current interest. Although ^{111}In labeled polyclonal IgG is probably the most widely cited protein being evaluated for focal infection scintigraphy (*1–4*), the mechanism of radiolabel accumulation remains unclear (*5–8*). In this issue of *The Journal of Nuclear Medicine*, Oyen et al. examined the roles of protein carrier and radiolabel in targeting of abscesses (*9*). They evaluated three different protein carriers and went on to assess the contribution of three different radiolabels and their associated chemistries in imaging experimental infectious foci in a rat model.

In the first part of the study, the authors compared radiolabeled IgG with immunoglobulin A (IgA) and human serum albumin (HSA) controls since these proteins lack specificity for abscess. In each case ^{111}In labeling via a bifunctional chelate served as the standard radiolabel so that localization differences could be ascribed to individual protein distribution properties. Layered upon the targeting properties of the protein was the contribution of the radiolabels and their chemistries. In the second part of the study, the authors compared various radiolabels with IgG serving as the standard protein vehicle.

This study was well-conceived and designed to determine the role of protein carrier and radiolabel. However, an accurate interpretion of the role of the protein assumes the radiolabel serves as a radiotracer. Furthermore, an interpretion of the role of the radiolabel requires an analysis of its chemistry and an appreciation for the pharmacokinetics of its radioactive metabolites. Since these properties direct the biodistribution of radioactivity, it is instructive to briefly review relevant factors such as attachment stability, metabolic fate, and route of excretion characteristic of radioiodines, ^{111}In and ^{99m}Tc as used in this study.

IODINE AS RADIOTRACER

Radioiodine isotopes continue to be the most widely used protein radiolabels: ^{123}I for imaging, and ^{125}I and ^{131}I for preclinical studies with their convenient longer half-lives and ready availability. The "easy" direct radioiodination approach in which the radioiodine is added to the activated ortho position of tyrosine is most often used, as was done in the Oyen et al. study (*9*). Label stability is usually sufficient to follow proteins in circulation or bound to cell surfaces. Once internalized by cells, however, catabolism releases peptide fragments or free amino acids with further metabolic processing ultimately releasing radioiodide (*10*). Deiodination may occur rapidly as in the example of the T-101 antibody in which imaging of cutaneous T-cell lymphoma is virtually precluded by rapid loss of radioactivity from tumor cells (*11*). Metabolically stabilized ligand chemistry has been developed which substan-

Received Dec. 10, 1991; accepted Dec. 12, 1991.
For reprints contact: Alan Fritzberg, NeoRx Corp., Seattle, WA 98119.